High-Throughput Screening of PLGA Thin Films Utilizing Hydrophobic Fluorescent Dyes for Hydrophobic Drug Compounds

TERRY W. J. STEELE,[1] CHARLOTTE L. HUANG,[1] SARANYA KUMAR,[1] EFFENDI WIDJAJA,[2] FREDDY YIN CHIANG BOEY,[1] JOACHIM S. C. LOO,[1] SUBBU S. VENKATRAMAN[1]

[1]Materials and Science Engineering, Division of Materials Technology, Nanyang Technological University, Singapore 639798

[2]Process Science and Modeling, Institute of Chemical and Engineering Sciences, Agency for Science, Technology and Research (A*STAR), Singapore 627833

Received 28 January 2011; revised 2 April 2011; accepted 26 April 2011

Published online 23 May 2011 in Wiley Online Library (wileyonlinelibrary.com). DOI 10.1002/jps.22625

ABSTRACT: Hydrophobic, antirestenotic drugs such as paclitaxel (PCTX) and rapamycin are often incorporated into thin film coatings for local delivery using implantable medical devices and polymers such as drug-eluting stents and balloons. Selecting the optimum coating formulation through screening the release profile of these drugs in thin films is time consuming and labor intensive. We describe here a high-throughput assay utilizing three model hydrophobic fluorescent compounds: fluorescein diacetate (FDAc), coumarin-6, and rhodamine 6G that were incorporated into poly(D,L-lactide-*co*-glycolide) (PLGA) and PLGA–polyethylene glycol films. Raman microscopy determined the hydrophobic fluorescent dye distribution within the PLGA thin films in comparison with that of PCTX. Their subsequent release was screened in a high-throughput assay and directly compared with HPLC quantification of PCTX release. It was observed that PCTX controlled-release kinetics could be mimicked by a hydrophobic dye that had similar octanol–water partition coefficient values and homogeneous dissolution in a PLGA matrix as the drug. In particular, FDAc was found to be the optimal hydrophobic dye at modeling the burst release as well as the total amount of PCTX released over a period of 30 days.
 J Pharm Sci 100:4317–4329, 2011

Keywords: PLGA; paclitaxel; drug delivery; high-throughput screening; Raman spectroscopy; fluorescein; thin films; polymers; surface analysis; scanning electron microscopy

INTRODUCTION

Paclitaxel (PCTX) is well described as an important treatment in various cancer pathologies including ovarian, breast, and lung cancers. A lesser known application for this compound is in treating cardiovascular disease, in particular limiting the growth of scar tissue, or restenosis. Drug-eluting stents have incorporated PCTX into the slow-release thin films, which confer reduced restenosis over several weeks.[1] The Taxus® stent, by Boston-Scientific (Natick, MA), is a commercial stent with a nonbiodegradable thin film coating on a stainless steel stent. It was initially well received, but was later associated with higher thrombosis rates compared with bare-metal stents.[2,3] Because of this detrimental effect, it has been proposed that localized delivery of PCTX immediately following percutaneous transluminal (coronary) angioplasty treatment, without stenting, should improve the long-term outcome of the procedure; favorable results in early clinical trials have justified this notion.[4,5] Various studies focused on producing PCTX incorporating thin films are presently under way. Films with release profiles that control the burst and extended dosages from weeks to months are being developed.[6–8] However, to date, there are no high-throughput methods to screen thin films for the release of PCTX and other hydrophobic drugs such as rapamycin and everolimus.

Correspondence to: Joachim S. C. Loo (Telephone: +65-6790-4603; Fax: +65-6790-9081; E-mail: joachimloo@ntu.edu.sgs)

Correspondence to: Subbu S. Venkatraman (Telephone: +65-6790-4259; Fax: +65-6790-9081; E-mail: assubbu@ntu.edu.sg)

Terry W. J. Steele and Charlotte L. Huang have contributed equally to this manuscript.

Journal of Pharmaceutical Sciences, Vol. 100, 4317–4329 (2011)

The gold standard technique of PCTX quantification has been high-performance liquid chromatography (HPLC) with C18 column separation and detection with ultraviolet (UV) absorbance ($\lambda_{max} = 227$ nm, $\varepsilon = 2.8 \times 10^4$ M^{-1} cm^{-1}). On optimized isocratic systems, individual analyses run under 10 min with limit of quantification at 0.05 μg/mL.[9] This is only seven times lower than the maximum solubility of PCTX in aqueous solutions.[10] To increase the solubility of PCTX, addition of organic solvents or surfactants was needed, thus complicating HPLC analyses.[11,12] The inefficient rate of sample throughput using HPLC is also a major flaw because the quantification of drug release by one HPLC apparatus is limited to a maximum rate of 10 thin film formulations per day. The extensive time required to complete HPLC analysis, including sample preparation, for a time course experiment with replicates restricts the number of films a worker can realistically study in a single session. It is therefore of great use to develop an approach toward quick turnover, bulk screening, allowing film optimization in substantially shorter time frame.

An alternative approach would be to use fluorescence spectroscopy, as this would avoid the most laborious preparation steps and thus speed up the quantification by orders of magnitude. Indeed, quantification by fluorescence in a 96-well plate takes seconds per sample compared with 10 min per sample in an HPLC. However, hydrophobic compounds such as PCTX and rapamycin are not fluorescent. Fluorescent analogues of these compounds do exist, for use in biochemistry mechanism investigations, wherein microgram quantities are required.[13] Currently, these fluorescent compounds are prohibitively expensive for use in the milligram to gram amounts needed in thin film extended-release preparations.

The next best option would be to acquire more economical hydrophobic fluorescent compounds that are suitable for screening the thin film formulations. These could be used to select best candidate film formulations from a larger panel, for further assessment using the more laborious HPLC hydrophobic drug quantification. The use of hydrophobic fluorescent compounds in place of hydrophobic drugs for visualization and tracking has been previously documented. For example, fluorescent Nile red was used in place of PCTX in poly (D,L-lactide-*co*-glycolide) (PLGA) nanoparticles to observe the nanoparticle cellular uptake and subsequent Nile red release.[14] Similar experiments with PLGA–montmorrillonite nanoparticles used coumarin-6 (structurally similar to Nile red) in place of PCTX for cellular uptake observations.[15]

In this investigation, a novel method of high-throughput quantification of the thin film drug release was optimized in the form of a 96-well plate assay. Three commercially available fluorescent compounds were chosen with similar hydrophobic properties to PCTX (octanol–water partition coefficient, log *P*, of 4.0–4.4; Refs.[16,17]) and compared against the release of PCTX in PLGA and PLGA–polyethylene glycol (PEG) films by HPLC methods. Table 1 shows the three hydrophobic fluorescent compounds: rhodamine 6G, fluorescein diacetate (FDAc), and coumarin-6, with log *P* values of 4.02, 4.2, and 5.43, respectively.[18–20] The fluorescent compounds were chosen due to their similar log *P* values to the drug, as earlier reports list the solubility in the PLGA matrix (dry or wet) as the predominant factor that influences the rate of delivery.[21] Molecular weight, molecular volume, and topological surface areas[22] are also listed for comparison of PCTX with the hydrophobic dyes.

MATERIALS AND METHODS

Materials

Poly (D,L-lactide-*co*-glycolide) 53/47 (PLGA with a 53/47 lactide–glycolide ratio) with intrinsic viscosity (i.v.) of 0.2 dL/g [~10 kDa molecular weight (MW)] and 1.03 dL/g (~100 kDa MW) was purchased from Purac (Gorinchem, Netherlands). PCTX was purchased from Yunnan Hande Bio-Tech (Kunming, China). HPLC-grade dichloromethane (DCM) and acetonitrile were purchased from Tedia (Singapore). Deuterated chloroform [$CDCl_3$ + 0.03%, v/v, tetramethylsilane (TMS) D99.8% + silver foil] was purchased from Cambridge Isotope Laboratories (Andover, Massachusetts). PEG of MW of 8000 and 35,000 Da and polysorbate 80 (Tween 80) were purchased from Sigma –Aldrich (Singapore). Rhodamine 6G, coumarin-6, and FDAc were purchased from TCI Japan (Singapore). All other polar solvents used were of HPLC grade and were supplied by Sigma–Aldrich. All chemicals and materials were used as received.

Film Formulation

Solutions of PLGA–PEG prepared at a concentration of 20% (w/v) (in DCM) were used to incorporate 10% (w/w) PCTX–fluorescent dye (PCTX–fluorescent dye in PLGA–PEG) in DCM. Hence, a typical film formulation consisted of 60 mg of PCTX–fluorescent dye and 600 mg of polymer (PLGA + 0%–50% PEG) in 3 mL of DCM. Such a preparation was carried out as follows: a 15% 8000 PEG–PLGA 53/47 solution was dissolved in 3 mL of DCM overnight with 60 mg of PCTX, 510 mg of PLGA 53/47 (i.v. 1.03 dL/g), and 90 mg of 8000 PEG.

Film casting was performed with the film applicator height set at 300 μm, and the viscous solution was cast onto 50 μm polyethylene teraphthalate substrate at 50 mm/s in a fume extractor hood at room temperature (RT). DCM was evaporated at RT for 24 h followed by at 55°C for 2 days in a vacuum oven.

Punch-outs of 6 mm diameter were prepared for release studies, with the PLGA films still mounted on the polyethylene teraphthalate substrate.

PEG Quantification by ^{1}H NMR

Films (1 cm^2) were dissolved in 1050 ± 10 μg (700 μL) of $CDCl_3$, mixed by vortexing, and centrifuged at 16,000xg for 5 min, the subsequent supernatant was transferred into NMR tubes. ^{1}H NMR spectra were recorded on Bruker Advance Spectrometer (Bruker Biospin PTE LTD, Singapore) at 400 MHz using the signal of TMS present in deuterated chloroform at 0.03% as an internal standard. ^{1}H NMR (400 MHz, CDCl3, δ) 1.5–1.7 [bs, PLGA 3H, −C(=O)−CH(C*H3*)−O−C(=O)−CH2−O−], 3.45–3.85 (bs, PEG 4H, −O−C*H2*C*H2*O−), 4.6–5.0 [bs, PLGA 2H, −C(=O)−CH(CH3)−O−C(=O)−C*H2*O−], 5.0–5.3 [bs, PLGA 1H, −C(=O)−C*H*(CH3)−O−C(=O)−CH2−O−].

Film Surface and Film Cross-section Topography by Scanning Electron Microscopy

Surface and cross-sectioned PEG-incorporated PCTX–PLGA films were coated with platinum for 50 s under a chamber pressure of less than 5 Pa at 20 mA using JEOL JFC-1600 Auto Fine Coater (JEOL ASIA PTE LTD, Singapore). Secondary electron images were acquired at 5.0 kV, 12 μA, at a working distance of 8 mm under the field emission scanning electron microscopy (FESEM) using a JEOL JSM-6340F (JEOL ASIA PTE LTD, Singapore). Film cross-sections were prepared by flash freezing the films in Tissue-Tek O.C.T. (Sigma-Aldrich, Singapore) compound at −80°C. Embedded film blocks were sliced while frozen at 10 μm and subsequently lyophilized under vacuum.

Raman Microscopy

Raman microscopy analysis has been performed as described earlier.[23] Briefly, the thin films were placed under the microscope objective and Raman point-by-point mapping measurements were performed on the sample. The sample was irradiated with a 785-nm near-infrared diode laser, and a 50× or 100× objective lens was used to collect the backscattered light. The collected Raman mapping spectra were then preprocessed (spike removal and baseline correction) before the data was further analyzed using the band-target entropy minimization (BTEM) algorithm. The BTEM algorithm[24] was used to reconstruct the pure component spectra of underlying constituents from a set of mixture spectra without recourse to any a prior known spectral libraries. This has been proven to be effective in reconstructing the pure component spectra of minor components.[25–27] When all normalized pure component spectra of all the underlying constituents have been reconstructed, the relative contributions of each constituent can be calculated by projecting them back onto the baseline-corrected and normalized data set. The spatial distribution of each underlying constituents is then generated.

High-throughput Screening of Fluorescent Dyes

The 6-mm diameter disks consisting of fluorescent dye incorporated into PLGA were immersed in 200 μL of phosphate buffered saline (PBS)/2% Tween 80 solution, within a 96-well Costar flat black polystyrene flat-bottom plate. Samples were assayed in pentaplicates and stored in an incubator at 37°C in between sampling events. For rhodamine 6G (excitation/emission wavelengths in nanometers, ex/em: 480/560) and coumarin-6 (ex/em: 465/505), 100 μL aliquot was drawn out of the release plate and placed into a separate black read plate. The read plate was diluted with another 100 μL of PBS 2%/Tween 80 and assayed using the Infinite M200 Tecan Microplate spectrofluorometer (Tecan Asia PTE LTD, Singapore). For FDAc, 20 μL of the aliquot was drawn out of the release plate and diluted with 180 μL of 100 mM NaOH in the read plate, immediately yielding fluorescein (ex/em: 490/520). The amount of hydrophobic dye released was quantitated using three calibration curves (with separate gain settings) spanning three orders of magnitude: 0.01–10 μg/mL. The release plate had the remaining solution carefully drawn out, and replaced with another 200 μL worth of PBS/2% Tween 80. Rhodamine 6G, coumarin-6, and FDAc all had solubilities of more than 100 μg/mL in PBS/2% Tween 80. Each well was flashed 25 times, with a 20 μs integration. The entire 96-well plate was measured in <5 min for three gain settings. Instrument gain settings were experimentally determined by calibrating 90% of the maximum fluorescent signal (50,000 fluorescent units) at the highest standard concentration for the high gain (0.01–0.1 μg/mL), medium gain (0.01–0.10 μg/mL), and low gain (1.00–10.0 μg/mL) standard concentration ranges. The gain settings were then subsequently used for all controlled-release fluorescent dye quantitation.

In Vitro Pctx Release

The *in vitro* release of PCTX was conducted in 2 mL of PBS/2% Tween 80 release buffer (pH 7.4) at 37°C, using 15 mm punch-outs in triplicate. At predetermine time-points, the buffer was removed and replaced with another 2 mL release buffer, thus maintaining sink conditions throughout the release. The withdrawn aliquots (or standards/dissolutions samples) were flushed through a 0.2-μm syringe filter directly into HPLC vials and immediately capped. The PCTX content was quantified with an Agilent Series 1100 HPLC (Agilent Technologies, Santa Clara,

Table 1. Properties of Hydrophobic Fluorescent Dyes and Paclitaxel (PCTX)

Hydrophobic Dye/Drug	Log *P*	Volume	TPSA[a]	Rate K[b] (%/Day)	Diffusion Coefficient (cm^2/s) in 0.2 dL/g i.v. PLGA 53/47	Rate K[b] (%/day)	Diffusion Coefficient (cm^2/s) in 1.03 dL/g i.v. PLGA 53/47	Structure	Molecular Weight (g/mol)
Coumarin-6	5.42	316	42	NA	NA	NA	NA	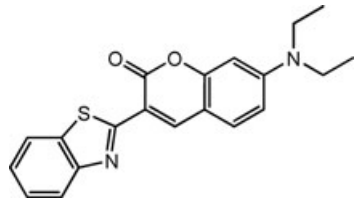	352
Fluorescein diacetate	4.20	365	88	4.04	$3.2\ e^{-5}$	1.07	$1.07\ e^{-5}$	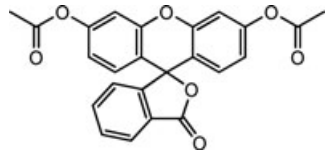	430
Rhodamine 6G	4.02	424	65	NA	NA	NA	NA	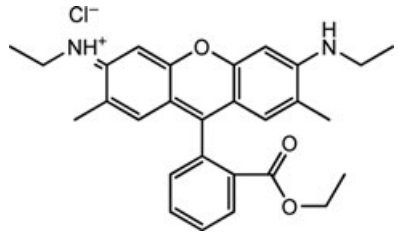	444
PCTX	4.0–4.4	757	221	4.4	$3.7\ e^{-5}$	1.6	$1.9\ e^{-5}$	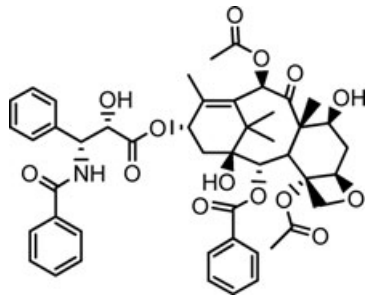	854

NA, not applicable due to incomplete dissolution of the hydrophobic dyes into the PLGA matrices.
ND, not determined; TPSA, topological polar surface area; PLGA, poly(D,L-lactide-*co*-glycolide); i.v., intrinsic viscosity.
[a]Volume ($Å^3$) and topological polar surface area ($Å^2$) were estimated using Cheminformatics.[22]
[b]Rate *K* and diffusion coefficients were calculated with a period of 12 days.

DOI 10.1002/jps

California) equipped with UV–visible (UV–Vis) detector, autosampler, and column heater set at 35°C. A ZORBAX Eclipse XDB-C18 (Agilent Technologies Singapore, Singapore) column (5 μm) of acetonitrile–water (60:40, v/v) served as the mobile buffer, eluting the PCTX peak at approximately 5.4 min with a flow rate of 1.0 mL/min and the UV–Vis detector recording at 227 nm. At the final end point, a total dissolution study of the 15-mm disks in triplicate was conducted by dissolving the films in acetone and diluting in release buffer to determine the surface concentration of PCTX (μg/mm^2). The solubility limit of PCTX in PBS/2% Tween 80 release buffer was determined to be 20 μg/mL (~50× that of PBS buffer).

RESULTS AND DISCUSSION

Thin Film Physical Properties

The method (viscous polymer solution knife casted on polyethylene terapthalate substrates) employed for film fabrication containing the PCTX and that for the hydrophobic dyes was identical. The analysis was optimized for using both HPLC PCTX quantitation and fluorescence measurements of the hydrophobic dyes. Figure 1 shows the film fabrication and analysis steps employed.

Initial analysis on the hydrophobic dyes and PCTX revealed that all four compounds were incorporated into two PLGA matrices of 0.2 and 1.03 dL/g i.v. In

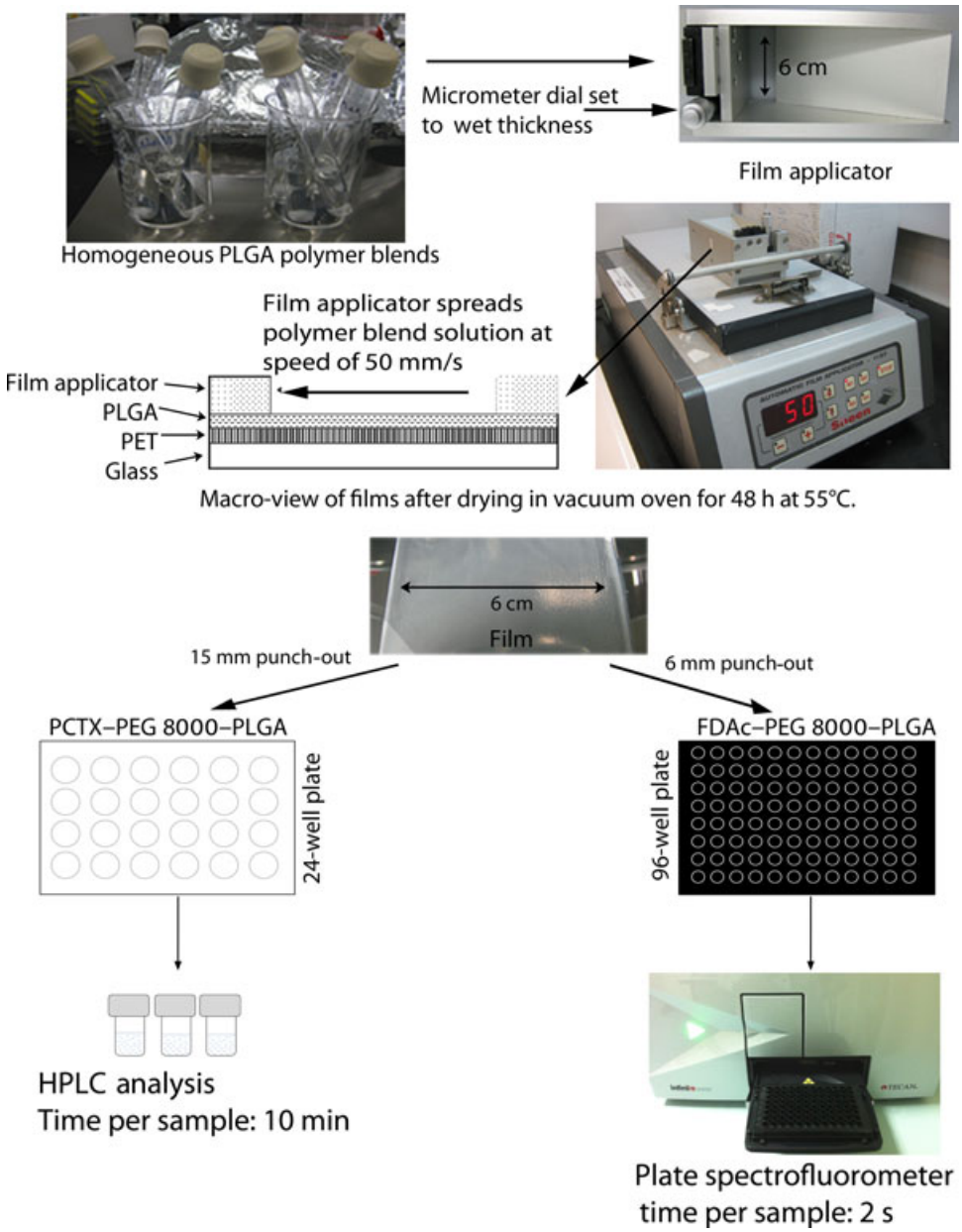

Figure 1. Scheme of PLGA thin film fabrication and analysis by HPLC or high-throughput 96-well plate spectrofluorometry.

Table 2. Physical Properties of Selected Paclitaxel and Fluorescein Diacetate Thin Films

Film Composition		Thickness	Drug Concentration	% PEG (by
Polymer[a]	Additives[b]	(μm)	(μg/mm^2)	^{1}H NMR)
PLGA 0.2 dL/g i.v.	10% FDAc	14 ± 2	4.3 ± 0.5*	0
PLGA 0.2 dL/g i.v.	10% PCTX	17 ± 3	6.4 ± 0.4*	0
PLGA 1.03 dL/g i.v.	10% FDAc	17 ± 3	4.5 ± 0.6	0
PLGA 1.03 dL/g i.v.	10% FDAc + 15% PEG 8000	17 ± 2	4.9 ± 0.4	16 ± 1
PLGA 1.03 dL/g i.v.	10% FDAc + 50% PEG 8000	13 ± 3	2.1 ± 0.3	50 ± 3
PLGA 1.03 dL/g i.v.	10% PCTX	16±2	4.2 ± 0.2	0
PLGA 1.03 dL/g i.v.	10% PCTX + 15% PEG 8000	16 ± 3	4.3 ± 0.8	16 ± 1
PLGA 1.03 dL/g i.v.	10% PCTX + 50% PEG 8000	13 ± 5	1.9 ± 0.2	50 ± 3

*Values are statistically different ($p < 0.05$).
PCTX, paclitaxel; FDAc, fluorescein diacetate; PEG, polyethylene glycol; i.v., intrinsic viscosity.
[a]PLGA, poly(D,L-lactide-*co*-glycolide) 53/47 (lactide–glycolide ratio) with different i.v. of 0.2 or 1.03 dL/g.
[b]All percentages are in w/w ratios.

addition, the four compounds were incorporated into PLGA (i.v. 1.03 dL/g) with two types of PEG MW at two (w/w) ratios: 8000 and 35,000 PEG at 15% and 50% (w/w) ratios each (Table 1). Table 2 displays the thin film values of thickness, surface drug concentration, and the percentage of PEG. Representative films from FDAc- and PCTX-containing films are shown, but similar values were seen for the fluorescent dyes of coumarin-6 and rhodamine 6G. The addition of large amounts of PEG (i.e., 50% formulations) yielded thinner viscosities in the DCM solutions, which subsequently generated thinner films and lower drug concentrations when dried. PCTX caused thicker films in the PLGA (i.v. 0.2 dL/g) films versus FDAc, although this was likely attributed to slight differences in film fabrication.

Although rarely reported for assessing PLGA films, we found that ^{1}H NMR analysis was a robust technique to analyze the matrix chemical composition. The percentage of PEG was verified and measured through the ^{1}H NMR PEG integrals present from 3.45 to 3.85 ppm, as seen in Figure 2. FDAc was an ideal candidate for ^{1}H NMR quantification as the two methyl esters (with six protons) had a strong singlet at 2.33 ppm. The DCM dissolved-knife cast films required 24 h of drying at atmospheric pressure before 55°C vacuum oven exposure. Without the 24 h of air drying, unpredictable foam matrices occurred

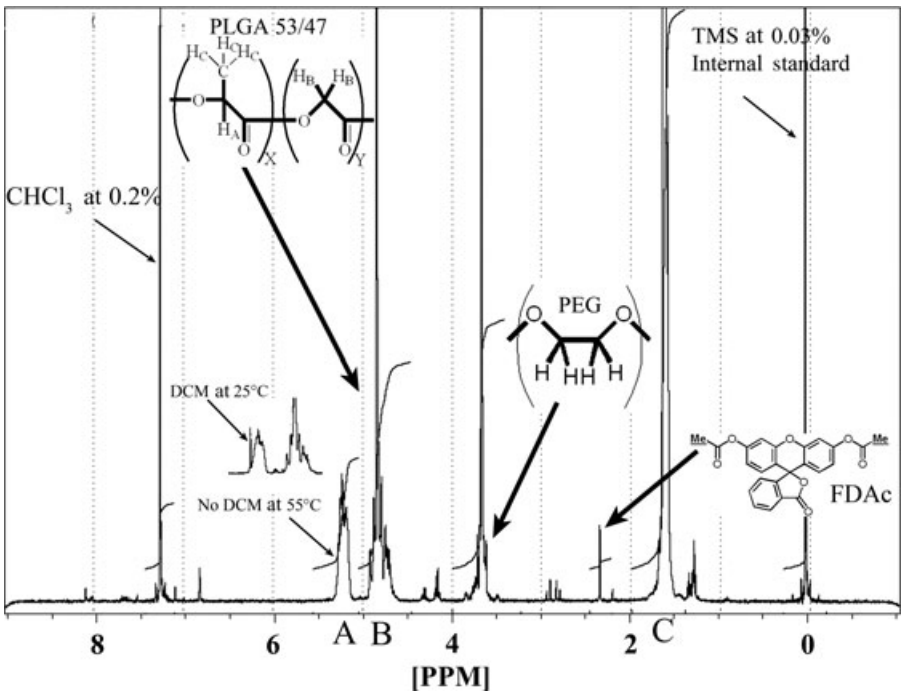

Figure 2. ^{1}H NMR of 15% 35,000 PEG–PLGA (53/47 with i.v. 1.03 dL/g) containing 10% fluorescein diacetate (FDAc). Tetramethylsilane (TMS) was used as the internal standard for ppm and ^{1}H quantification. (Inset) Presence of Dichloromethane (DCM) peak after 48 h vacuum oven drying at 25°C, but not at 55°C.

(data not shown). Higher boiling point solvents were avoided in this study because longer incubations at atmospheric pressures would be needed. The optimized drying procedure employed a vacuum oven at 55°C after RT drying, which yielded less than 500 ppm and less than 3 μg residual DCM, for an assumed 5 mg PLGA film (Fig. 1 inset displays the ^{1}H NMR DCM peaks at two drying conditions). It may be noted that this level falls under US Food and Drug Administration guidelines of <600 ppm and <6 mg/day residual DCM.[28]

The cross-section and surface topology of the PLGA films were analyzed using FESEM at 700× magnification. Figure 3 shows a representative photograph of PLGA (53/47 with i.v. of 1.03 dL/g) with 10% drug encapsulation (no PEG additives). At day 0, a solid matrix was seen with no pores present at the surface. After 10 days in release buffer, pore formation on the surface and within the matrix cross-section displayed a porous film that had swelled to almost twice its original thickness (~25 μm). The uniform degradation from the top to the bottom surface suggests bulk degradation with no autocatalytic processes occurring. Autocatalytic degradation tends to display a more degraded core than film surface and is usually noted only in films thicker than 200 μm.[29] The effect of combining PEG with PLGA (53/47 with i.v. of 1.03 dL/g) and subsequent degradation has previously been discussed.[23]

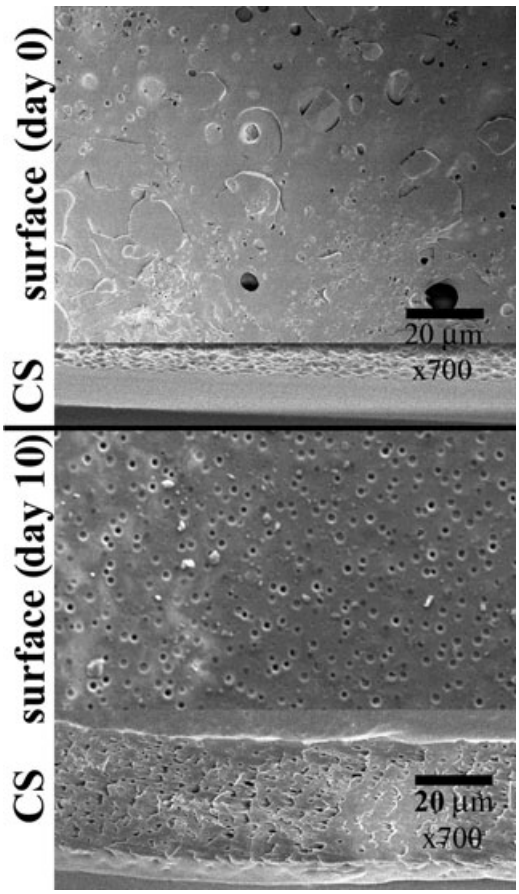

Figure 3. Cross-section and surface topology of PLGA (53/47 with i.v. 1.03 dL/g) containing 10% FDAc films at day 0 (top) and day 10 (bottom) incubation in release buffer. Images were taken at 700× magnification on a field emission scanning electron microscopy (JEOL JSM-6340F).

PLGA Film Characterization by Raman Microscopy: Partitioning of the Hydrophobic Dyes and Paclitaxel

In earlier work, we demonstrated with the use of Raman microscopy, how the presence of colocalized PCTX in crystalline PEG (vs. amorphous PEG) can affect the overall drug release from PLGA films.[23] Furthermore, Raman peaks of crystalline PEG at 844 and 860 cm^{-1} have been previously used to differentiate the PEG crystalline phase from its amorphous phase.[30] The Raman peak assignments for all the compounds tested are shown in Table 3. When PCTX was distributed homogeneously (see Figs. 4a and 4b), the controlled release was slow [<2 μg/(cm^2 day)]. Depending on the MW, increasing the amount of PEG caused localized phase separations of crystalline PEG, as shown in Figure 4c with 15% 35,000 PEG in PLGA 53/47. PCTX preferentially colocalizes in these phase-separated crystalline PEG regions, and was subsequently released rapidly with the dissolved PEG. Hydrophobic dyes would require similar partitioning behavior to mimic the PCTX release. Coumarin-6 and rhodamine 6G were found to be heterogeneous even in PLGA 53/47 films without PEG. Upon drying the films, crystalline regions of coumarin-6 and rhodamine 6G were visualized with the naked eye and confirmed with Raman microscopy.

Figure 4d shows an example of coumarin-6 analyzed by Raman microscopy. Phase separation of the crystalline coumarin-6 within the PLGA matrix region (bottom and top of color map, respectively, in Fig. 3d) was readily detectable. FDAc films exhibited homogeneous distribution for PLGA 53/47 (data not shown), with 15% PEG (both 8000 and 35,000 MW). A representative image of the FDAc distribution within 15% 35,000 MW PEG is shown in Figure 4e. FDAc in these three films was assumed to be dissolved completely in the PLGA 53/47 matrix, as the Raman signals were weak. At the highest concentration of PEG (50% of 8000 and 35,000 MW), a slight amount of FDAc–crystalline PEG colocalization occurred. However, a more pronounced colocalization of PCTX–crystalline PEG was present at 15% PEG than the FDAc–crystalline PEG at 50% (Figs. 4c vs. 4e). In general, the FDAc was distributed evenly within the film, regardless of crystalline–amorphous PEG and PLGA 53/47 phase separations.

Table 3. Raman Microscopy Peaks of Analyzed Compounds

Compound	Prominent Raman Peaks (cm^{-1})	Minor Raman Peaks (cm^{-1})
PLGA (53/47)	846, 873, 890	1046, 1095, 1130, 1425, 1454, 1768
Amorphous PEG	1231, 1278, 1469, 1479, 1486	582, 859, 1139, 1395
Crystalline PEG	844, 860	363, 534, 1063, 1124, 1140, 1280
Paclitaxel	1002	618, 1028, 1602
Fluorescein diacetate	658, 709,791, 1021, 1604, 1757	326, 449, 482, 530, 719, 734, 768, 844, 872, 1152, 1175, 1221, 1228, 1242, 1264, 1326
Coumarin-6	1435, 1481, 1512, 1587	474, 510, 629, 681, 700, 982, 1014, 1065, 1080, 1127, 1194, 1297, 1322, 1350, 1359, 1369, 1455, 1548
Rhodamine 6G	612, 770, 1313, 1365, 1511	873, 1128, 1182, 1451, 1650

Raman peaks of crystalline PEG at 844 and 860 cm^{-1} have been previously used to differentiate the PEG crystalline phase from its amorphous phase (Maxfield and Shepherd[30]).

Assay Sensitivity Using 96-well Plate/M200 Tecan Spectrofluorometer

The most convincing arguments for switching from the HPLC to a 96-well plate/fluorescence assay was the savings on labor, consumables cost, and increased method sensitivity. The specifications of the M200 spectrofluorometer allowed for the sensitivity of fluorescein detection/quantification in 96-well plates to be within the picomolar range. The instrument has the capability of 20 s/plate read throughput,[31] although in practice, we found it ranged from 1 to 2 min/plate at a single gain and excitation–emission setting. Linear curves down to 1 ng/mL (~4 nM) fluorescein were easy to reproduce. Quantification in this range was important for experimental use in *in vivo* formulations and for *ex vivo* bioreactors, wherein thin films often release encapsulated drugs into liters of medium.

Fluorescein was best read at high pH values, as high pH instantly cleaves the esters present in nonfluorescent FDAc to the fluorescent form. This allowed it to be utilized in the cells and vesicles as a "pH meter."[32] Indeed, we found that small changes in physiological pH (±0.04 pH units) caused an increase in fluorescence unit standard deviation. At basic pH of approximately 12–13, fluorescence was at its brightest and did not show an increase in standard deviation (data not shown). Fluorescent dyes coumarin-6 and rhodamine 6G did not show this pH-dependent fluorescence fluctuation, and were measured at pH 7.4. Average plate read time was approximately 4.5 min for all three fluorescent dyes, using following three gain settings: high gain, 0.01–0.10 μg/mL; medium gain, 0.10–1.0 μg/mL; and low gain, 1.0–10.0 μg/mL.

Release in Fast (i.v. 0.2 dL/g) and Slow (i.v. 1.03 dL/g) Degrading PLGA Thin Films

To mimic the *in vivo* solubility conditions for PCTX, *in vitro* release conditions were modulated using 2% Tween 80 in PBS buffer at 37°C. The addition of 2% Tween 80 allows soluble PCTX concentrations of 20 μg/mL, 50 times that of PBS alone and equivalent to albumin-bound blood concentrations.[33] Tween 80 has commonly been used to dissolve PCTX for this purpose,[34,35] and allowed solutions of more than 100 μg/mL concentrations of the fluorescent compounds to be prepared (data not shown).

The drug release behavior of the hydrophobic fluorescent molecules FDAc, coumarin-6, rhodamine 6G, and PCTX revealed diffusion-controlled release in all of the pure PLGA films at i.v. of 0.2 and 1.03 dL/g. The FDAc and PCTX revealed a similar drug release profile with no burst release. With similar log *P* values and homogeneous (also known as amorphous) PLGA matrix distribution, this was to be expected. Rhodamine 6G and coumarin-6 displayed higher burst release, likely due to the phase separated, crystalline state of the two dyes within the matrix. At the 10% (w/w) concentration, rhodamine 6G and coumarin-6 were not completely soluble within the PLGA matrix

The structures of rhodamine 6G and coumarin-6 (see Table 1) may explain why they were insoluble at 10% (w/w) in PLGA. Even though these molecules have a hydrophobic log *P* similar to PCTX, their amine substituents provide a local polar behavior that decreased their solubility in the hydrophobic PLGA matrix. This effect was unexpected because coumarin-6 substitution for PCTX was common for previous cell uptake and imaging studies, although these used smaller (w/w) concentrations.[15,36]

The controlled release of the four compounds was then compared across two MW neat PLGAs at i.v. 0.2 and 1.03 dL/g in Figures 5a and 5b. The 0.2 dL/g i.v. PLGA matrices revealed a faster dye and PCTX release than i.v. of 1.03 dL/g in PLGA. At the higher i.v. (and MW), the longer and less soluble polymer chains slowed the diffusion rate of the drugs. Larger PLGA chains tend to retain more of the encapsulated dye and for longer.[37] Coumarin-6, FDAc, and PCTX had roughly twice the release kinetics at i.v. 0.2 dL/g as that at i.v. 1.03 dL/g PLGA. Rhodamine 6G exhibited a gradual release in i.v. 0.2 dL/g PLGA, whereas the i.v. 1.03 dL/g PLGA gave an abrupt release from 20 to 25 days.

Overall, FDAc was found to mimic the PCTX release kinetics the most. On the basis of the equations

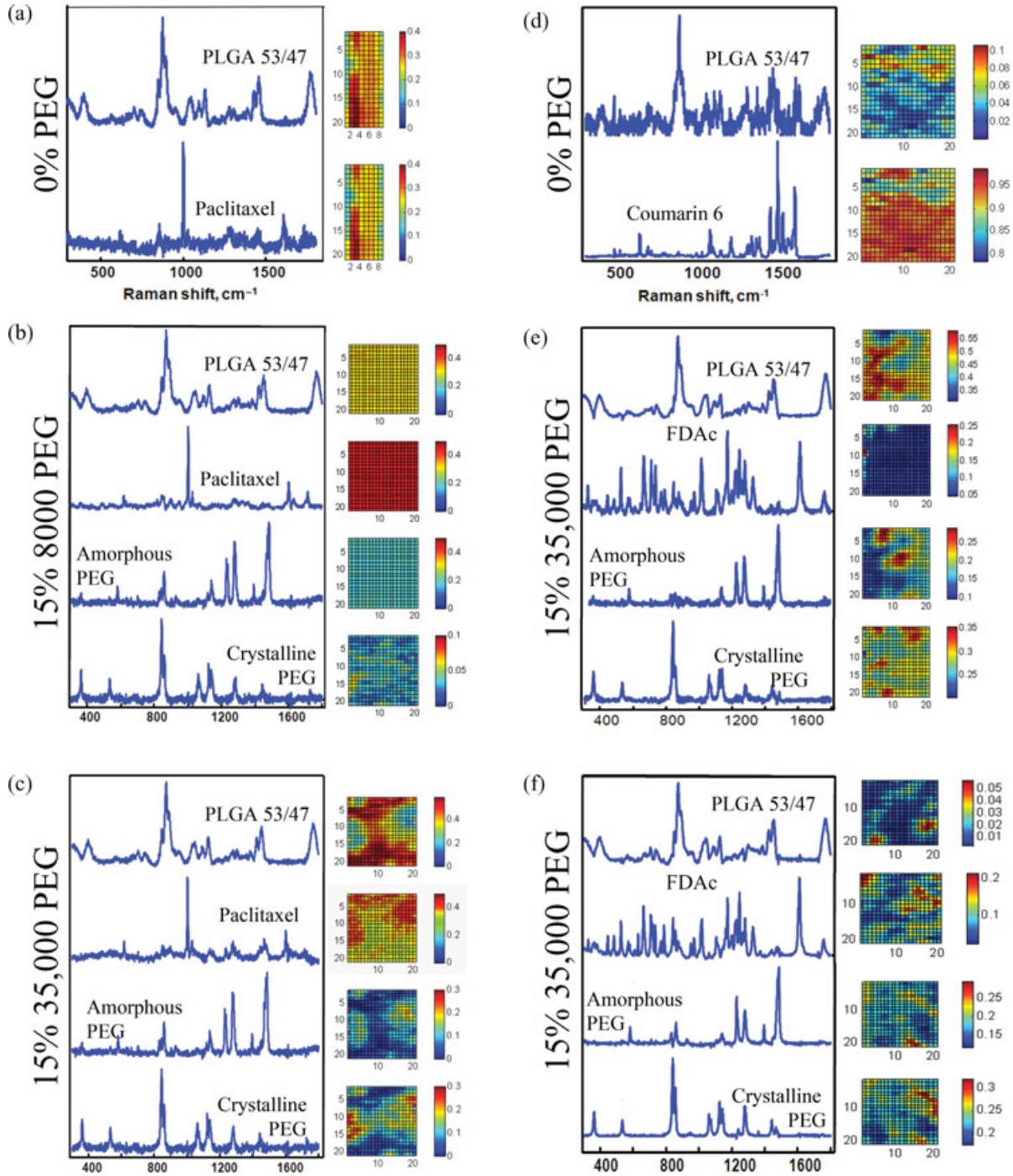

Figure 4. Raman microscopy of selected PLGA 53/47 (neat) and PLGA 53/47 with PEG films containing 10% (w/w) hydrophobic dyes and paclitaxel (PCTX). (a) PLGA 53/47 with 10% PCTX; (b) PLGA 53/47, 15% 8000 PEG, and 10% PCTX; (c) PLGA 53/47, 15% 35,000 PEG, and 10% PCTX; (d) PLGA 53/47 with 10% coumarin-6; (e) PLGA 53/47, 15% 35,000 PEG, and 10% fluorescein diacetate (FDAc); and (f) PLGA 53/47, 50% 35,000 PEG, and 10% FDAc.

of the semiemperical Power Law, rate K and the diffusion coefficients were calculated and listed in Table 1, allowing a comparison between PCTX and FDAc.[38] Despite PCTX almost having twice the molecular volume of FDAc (see Table 1), the diffusion coefficients were comparable for both i.v. 0.2 and 1.03 dL/g PLGA matrices.

Release in Low and High Percentage PLGA Additives Using 8000 and 35,000 MW PEG

The drug release behavior of PCTX and hydrophobic dyes FDAc, coumarin-6, and rhodamine 6G also showed diffusion-controlled release with the addition of PEG additives at PLGA i.v. of 1.03 dL/g. Distinct

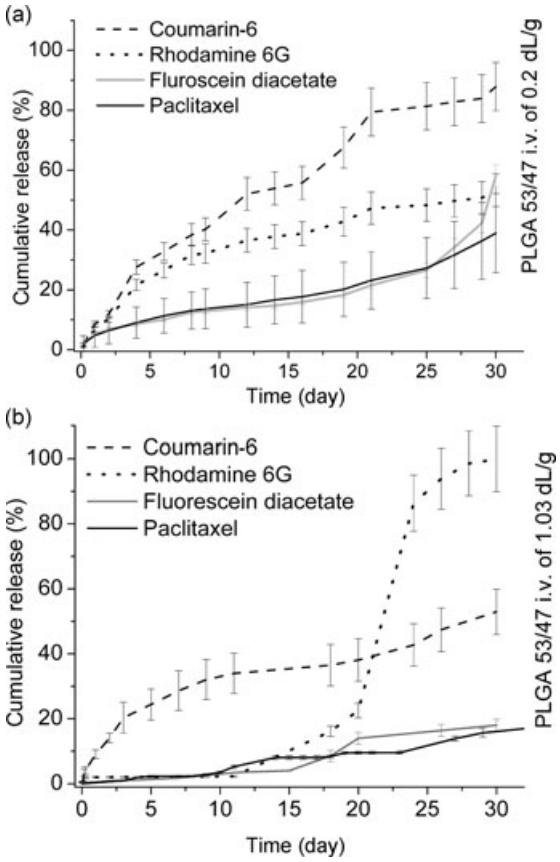

Figure 5. Slow and fast release of hydrophobic fluorescent dyes and in 0.2 (a) and 1.03 dL/g (b) i.v. PLGAs.

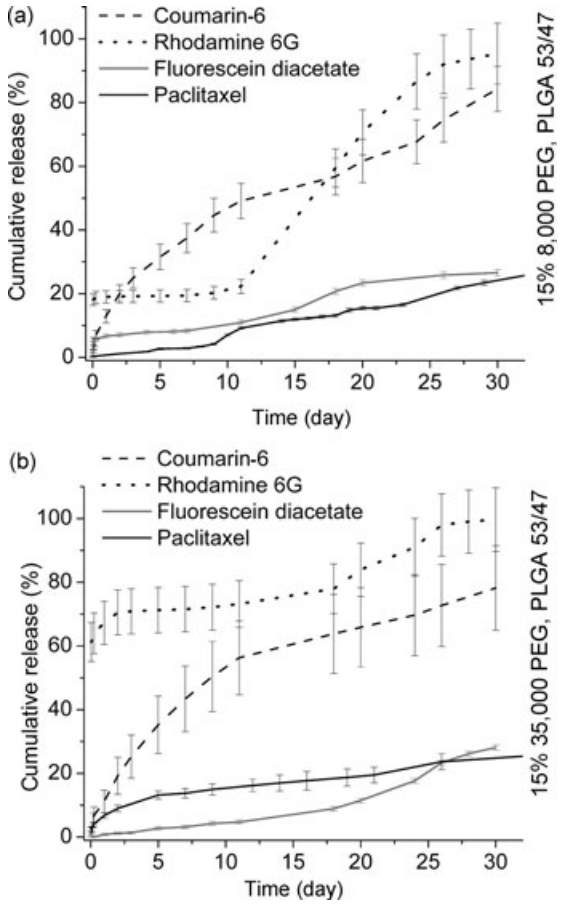

Figure 6. Low percentage additive release using (a) 15% 8000 MW PEG and (b) 15% 35,000 MW PEG.

observation can be made from the release profiles shown in Figures 6a and 6b, whereby, from the drug panel, only rhodamine 6G exhibited a burst release of 20% and 60%, respectively, from PLGA with 15% 8000 and 35,000 PEG,. Hence, an increased burst release occurs with larger PEG MW additive. In addition, an increase in the percentage of PEG additive also causes greater burst release. These two effects are confirmed by the highest burst release being detected in PLGA incorporated with PEG 35,000 at 50% (w/w) concentration; that is, the highest MW and percentage additive tested (Fig. 7). Such a large burst release could be partly attributed to the following: lower log *P* value in rhodamine 6G, ionic molecule formation in solution, crystalline phase separation, or combination thereof. In the case of coumarin-6, it is assumed that the crystalline phase separation accounts for the higher rate of release observed as well.

The subsequent controlled releases of the four dyes were then further compared across two MW PEG additives of 8000 and 35,000 at two percentages, that is, 15% and 50% (Figs. 6 and 7). The larger 35,000 MW PEG generally gave a smaller percentage of burst release as compared with 8000 MW PEG at 50% concentration (Fig. 7). An increase in colocalization of the larger MW PEG (analyzed for FDAc and PCTX) resulted in a sustained release. PCTX is known to colocalize with PEG chains via intercalating chemistry due to its aromatic rings.[39] Such an occurrence may also be expected for the three fluorescent dyes. A higher concentration of PEG at 50% gave an increased rate of release compared with 15% PEG, as deduced from the steeper release curve over the initial days of the release profile. The steeper curve results from the PEG dissolution and leaching.[23] As the greater colocalization was likely associated with higher PEG concentrations, an increased release was therefore expected to occur for all drug molecules at high PEG content.

FDAc as a Model Hydrophobic Drug for Screening Thin Film Preparations

The release profile of FDAc was found to have a good correlation with that of PCTX when encapsulated within pure PLGA films. This was found to be independent of the two MW PLGA matrices shown in Figure 5. The release of FDAc only began to differ from PCTX upon addition of PEG, an additive that was known to phase-separate within PLGA (see Figs. 6 and 7). Within these heterogeneous films, our

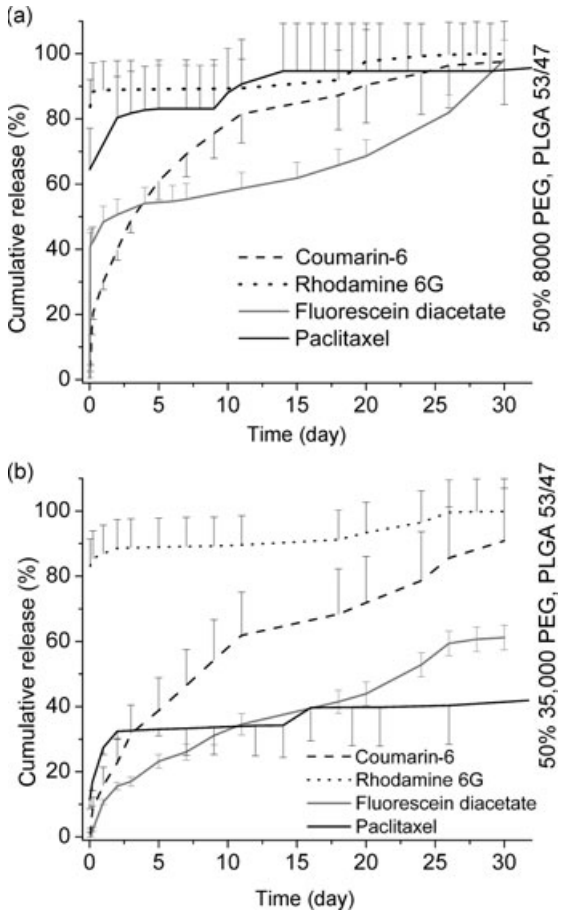

Figure 7. High percentage additive release using (A) 50% 8000 MW PEG and (B) 50% 35000 MW PEG. Some error bars have been removed for clarity.

hypothesis of mimicking the PCTX log *P* with a similar hydrophobic fluorescent compound was no longer valid. Log *P* only predicts preference toward hydrophobic solvents (or PLGA matrices) in contact with in an aqueous phase. It cannot provide any information toward tertiary amphiphilic compounds such as PEG that phase-separate within the PLGA. Fortunately, these phase separations were typically easy to visualize by the naked eye, light microscopy, Raman microscopy, or combination thereof. A quick assessment of the homogeneous structure by these techniques will decide whether this high-throughput method may be of use.

The differences in FDAc and PCTX distribution among PEG and PLGA described here may be explained with another solubility descriptor, topological polar surface area (TPSA, listed in Table 1). TPSA represents the sum of polar surfaces of nitrogen, oxygen, and their bound hydrogen atoms. It has proved to be a useful parameter for drug transport analysis in intestinal and blood–brain barrier absorption.[22] Within the context of our experiments, higher TPSA was associated with PEG partitioning. The lowest TPSA values were observed with coumarin-6 and rhodamine 6G; no PEG partioning was detected in the PLGA films with either of these two molecules. The second highest TPSA value was for FDAc with 88 $Å^2$, which had a minor partioning at the highest 50% PEG concentration. PCTX was present with the most amount of crystalline PEG partioning and had greater than twofold TPSA of FDAc with 221 $Å^2$.

CONCLUSIONS

Three fluorescent dyes with log *P*s similar to PCTX have been evaluated in PLGA films with Raman microscopy for molecular distribution and compared against PCTX release of less than 30 days. Two of the dyes, rhodamine 6G and coumarin-6, were found to be inadequate, as they were not soluble within the PLGA matrix, and tended to be phase separated and crystallized. One hydrophobic dye, FDAc (converted to fluorescein when treated with base), was found to be a model drug toward estimating the PCTX release profile. It displayed similar diffusion coefficients in homogeneous PLGA films (i.v. of 0.2 and 1.03 dL/g). When PEG additives were present, FDAc was still found to mimic the PCTX release, when phase separation was not substantial. As the MW and concentration of PEG increased, more crystalline PEG phase separation was present. Under these conditions, PCTX preferentially colocalized into the crystalline PEG more than the FDAc, with varying release profiles. If phase-separating additives are introduced, alternative drug models need to be considered.

This report demonstrates that FDAc encorporation into PLGA can be controlled to model that of PCTX inclusion. Thus, a method for high-throughput screening of PLGA thin film formulations has been presented. With the use of FDAc in place of PCTX, fluorescent 96-well or possibly 384-well plate readers can be used while reducing the amount of consumables and decreasing the dependency for HPLC quantitation. We recommend the following guidelines for those who are considering this method:

(1) FDAc, PCTX, additives, and polymer matrix (i.e., PLGA or other polyester matrices) need to have similar hydrophobic properties to make homogeneous films.
(2) Visualization by light microscopy or Raman microscopy to assess microstructure for additive or drug phase-separated regions.
(3) Polymer films thicknesses should be similar and less than 200 μm to avoid autocatalytic degradation effects.
(4) This method should be considered when multiple formulations (≥10 thin films) need to be simultaneously screened for PCTX delivery. When testing less than 10 films overall, the time

saved by this fluorescence protocol does not justify the need for preparation of separate FDAc-containing films.

(5) Applicable to studies when the drug release period is less than 30 days.

ACKNOWLEDGMENTS

The authors acknowledge and appreciate the help and support rendered by Dr. Scott A. Irvine, Ng Soon Ping, Goh Chye Loong Andrew, and Teo Guo Shun Eugene. Financial support was kindly given by NRF 2007 NRF-CRP 002-12 grant "Biodegradable Cardiovascular Implants."

Authors' contribution: Terry W. J. Steele, Charlotte L. Huang, and Joachim S. C. Loo designed the research. Terry W. J. Steele, Charlotte L. Huang, Saranya Kumar, and Effendi Widjaja performed the research. Terry W. J. Steele, Charlotte L. Huang, Effendi Widjaja, Joachim S. C. Loo, and Subbu S. Venkatraman analyzed the data. Terry W. J. Steele, Charlotte L. Huang, and Saranya Kumar wrote the paper. Freddy Yin Chiang Boey, Joachim S. C. Loo, and Subbu S. Venkatraman gave final approval for submission.

REFERENCES

1. Heldman AW, Cheng L, Jenkins GM, Heller PF, Kim DW, Ware M Jr, Nater C, Hruban RH, Rezai B, Abella BS, Bunge KE, Kinsella JL, Sollott SJ, Lakatta EG, Brinker JA, Hunter WL, Froehlich JP. 2001. Paclitaxel stent coating inhibits neointimal hyperplasia at 4 weeks in a porcine model of coronary restenosis. Circulation 103(18):2289–2295.
2. Lagerqvist B, James SK, Stenestrand U, Lindback J, Nilsson T, Wallentin L. 2007. Long-term outcomes with drug-eluting stents versus bare-metal stents in Sweden. N Engl J Med 356(10):1009–1019.
3. Galloe AM, Thuesen L, Kelbaek H, Thayssen P, Rasmussen K, Hansen PR, Bligaard N, Saunamaki K, Junker A, Aaroe J, Abildgaard U, Ravkilde J, Engstrom T, Jensen JS, Andersen HR, Botker HE, Galatius S, Kristensen SD, Madsen JK, Krusell LR, Abildstrom SZ, Stephansen GB, Lassen JF. 2008. Comparison of paclitaxel- and sirolimus-eluting stents in everyday clinical practice: The SORT OUT II randomized trial. JAMA 299(4):409–416.
4. Tepe G, Schmitmeier S, Speck U, Schnorr B, Kelsch B, Scheller B. 2010. Advances on drug-coated balloons. J Cardiovasc Surg (Torino) 51(1):125–143.
5. Unverdorben M, Kleber FX, Heuer H, Figulla HR, Vallbracht C, Leschke M, Cremers B, Hardt S, Buerke M, Ackermann H, Boxberger M, Degenhardt R, Scheller B. 2010. Treatment of small coronary arteries with a paclitaxel-coated balloon catheter. Clin Res Cardiol 99(3):165–174.
6. Chia NK, Venkatraman SS, Boey FY, Cadart S, Loo JS. 2008. Controlled degradation of multilayered poly(lactide-co-glycolide) films using electron beam irradiation. J Biomed Mater Res A 84(4):980–987.
7. Wang XT, Venkatraman S, Boey F, Loo SC, Tan LP. 2007. Effects of controlled-released sirolimus from polymer matrices on human coronary artery smooth muscle cells. J Biomater Sci Polym Ed 18(11):1401–1414.
8. Loo SC, Tan ZY, Chow YJ, Lin SL. Drug release from irradiated PLGA and PLLA multi-layered films. J Pharm Sci 99(7):3060–3071.
9. Mohammadi A, Esmaeili F, Dinarvand R, Atyabi F, Walker RB. 2009. Development and validation of a stability-indicating method for the quantitation of paclitaxel in pharmaceutical dosage forms. J Chromatogr Sci 47(7):599–604.
10. Hamada H, Ishihara K, Masuoka N, Mikuni K, Nakajima N. 2006. Enhancement of water-solubility and bioactivity of paclitaxel using modified cyclodextrins. J Biosci Bioeng 102(4):369–371.
11. Alexis F, Venkatraman SS, Rath SK, Boey F. 2004. In vitro study of release mechanisms of paclitaxel and rapamycin from drug-incorporated biodegradable stent matrices. J Control Release 98(1):67–74.
12. Yang T, Cui FD, Choi MK, Cho JW, Chung SJ, Shim CK, Kim DD. 2007. Enhanced solubility and stability of PEGylated liposomal paclitaxel: In vitro and in vivo evaluation. Int J Pharm 338(1–2):317–326.
13. Han Y, Chaudhary AG, Chordia MD, Sackett DL, Perez-Ramirez B Kingston DG, Bane S. 1996. Interaction of a fluorescent derivative of paclitaxel (Taxol) with microtubules and tubulin–colchicine. Biochemistry 35(45):14173–14183.
14. Xu P, Gullotti E, Tong L, Highley CB, Errabelli DR, Hasan T, Cheng JX, Kohane DS, Yeo Y. 2009. Intracellular drug delivery by poly(lactic-co-glycolic acid) nanoparticles, revisited. Mol Pharm 6(1):190–201.
15. Dong Y, Feng SS. 2005. Poly(d,l-lactide-co-glycolide)/montmorillonite nanoparticles for oral delivery of anticancer drugs. Biomaterials 26(30):6068–6076.
16. Forrest ML, Yanez JA, Remsberg CM, Ohgami Y, Kwon GS, Davies NM. 2008. Paclitaxel prodrugs with sustained release and high solubility in poly(ethylene glycol)-b-poly(epsilon-caprolactone) micelle nanocarriers: Pharmacokinetic disposition, tolerability, and cytotoxicity. Pharm Res 25(1):194–206.
17. Liu J, Lee H, Huesca M, Young A, Allen C. 2006. Liposome formulation of a novel hydrophobic aryl-imidazole compound for anti-cancer therapy. Cancer Chemother Pharmacol 58(3):306–318.
18. Cheruvu NP, Kompella UB. 2006. Bovine and porcine transscleral solute transport: Influence of lipophilicity and the Choroid–Bruch's layer. Invest Ophthalmol Vis Sci 47(10):4513–4522.
19. Lombry C, Bosquillon C, Preat V, Vanbever R. 2002. Confocal imaging of rat lungs following intratracheal delivery of dry powders or solutions of fluorescent probes. J Control Release 83(3):331–341.
20. Wright KM, Horobin RW, Oparka KJ. 1996. Phloem mobility of fluorescent xenobiotics in *Arabidopsis* in relation to their physicochemical properties. J Exp Bot 47(11):1779–1787.
21. Makoto Miyajima∗ AK, Jun'ichi Okada, Akira Kusai, Masaru Ikeda. 1998. The effects of drug physico-chemical properties on release from copoly (lactic/glycolic acid) matrix Int J Pharm 169(2):255–263.
22. Cheminformatics M. 2010. Molinspiration. http://www.molinspiration.com. Accessed December 30th, 2010.
23. Steele T, Huang C, Widjaja E, Loo J, Venkatraman S. 2011. The effect of polyethylene glycol structure on paclitaxel drug release and mechanical properties of PLGA thin films. Acta Biomater 7(5):1973–1983.
24. Widjaja E, Li C, Chew W, Garland M. 2003. Band-target entropy minimization. A robust algorithm for pure component spectral recovery. Application to complex randomized mixtures of six components. Anal Chem 75(17):4499–4507.
25. Widjaja E, Seah RK. 2008. Application of Raman microscopy and band-target entropy minimization to identify minor components in model pharmaceutical tablets. J Pharm Biomed Anal 46(2):274–281.

26. Widjaja E, Garland M. 2008. Use of Raman microscopy and band-target entropy minimization analysis to identify dyes in a commercial stamp. Implications for authentication and counterfeit detection. Anal Chem 80(3):729–733.
27. Seah RK, Garland M, Loo JS, Widjaja E. 2009. Use of Raman microscopy and multivariate data analysis to observe the biomimetic growth of carbonated hydroxyapatite on bioactive glass. Anal Chem 81(4):1442–1449.
28. FDA. 2003. Guidance for industry: Q3C—tables and list. http://www.fda.gov. Accessed on December 30th, 2010
29. Lu L, Garcia CA, Mikos AG. 1999. In vitro degradation of thin poly(DL-lactic-co-glycolic acid) films. J Biomed Mater Res 46(2):236–244.
30. Maxfield J, Shepherd I. 1975. Conformation of poly(ethylene oxide) in the solid state, melt, and solution measured by Raman scattering. Polymer 16:505–509.
31. Tecan. 2009. Tecan M200 multimode manual.
32. Chen Y, Arriaga EA. 2006. Individual acidic organelle pH measurements by capillary electrophoresis. Anal Chem 78(3):820–826.
33. Lovich MA, Creel C, Hong K, Hwang CW, Edelman ER. 2001. Carrier proteins determine local pharmacokinetics and arterial distribution of paclitaxel. J Pharm Sci 90(9):1324–1335.
34. Kang Y, Yin G, Ouyang P, Huang Z, Yao Y, Liao X, Chen A, Pu X. 2008. Preparation of PLLA/PLGA microparticles using solution enhanced dispersion by supercritical fluids (SEDS). J Colloid Interface Sci 322(1):87–94.
35. Jauhari S, Dash AK 2006. A mucoadhesive in situ gel delivery system for paclitaxel. AAPS PharmSciTech 7(2):E53.
36. Liu Y, Pan J, Feng SS. Nanoparticles of lipid monolayer shell and biodegradable polymer core for controlled release of paclitaxel: Effects of surfactants on particles size, characteristics and in vitro performance. Int J Pharm 395(1–2):243–250.
37. Korber M. 2010. PLGA erosion: Solubility- or diffusion-controlled? Pharm Res 27(11):2414-2420.
38. Baker R. 1987. Diffusion-controlled systems. New York: John Wiley & Sons.
39. Kang E, Robinson J, Park K, Cheng JX. 2007. Paclitaxel distribution in poly(ethylene glycol)/poly(lactide-co-glycolic acid) blends and its release visualized by coherent anti-Stokes Raman scattering microscopy. J Control Release 122(3):261–268.